HHS Public Access

Author manuscript

Meteorol Appl. Author manuscript; available in PMC 2024 November 16.

Published in final edited form as:

Meteorol Appl. 2023 ; 30(1): . doi:10.1002/met.2112.

Verification of operational numerical weather prediction model forecasts of precipitation using satellite rainfall estimates over Africa

Yan Wang[1], **Moussa Gueye**[1,2], **Steven J. Greybush**[1,3], **Helen Greatrex**[3,4], **Andrew J. Whalen**[5,6], **Paddy Ssentongo**[5,7], **Fuqing Zhang**[1,†], **Gregory S. Jenkins**[1], **Steven J. Schiff**[3,5,8,9]

[1]Department of Meteorology and Atmospheric Science, The Pennsylvania State University, University Park, Pennsylvania, USA

[2]Department of Mathematics and Computer Sciences, Université du Sine Saloum El Hadji Ibrahima Niass (USSEIN), Kaolack, Senegal

[3]Institute for Computational and Data Sciences, The Pennsylvania State University, University Park, Pennsylvania, USA

[4]Department of Geography and Department of Statistics, The Pennsylvania State University, University Park, Pennsylvania, USA

[5]Center for Neural Engineering and Center for Infectious Disease Dynamics, The Pennsylvania State University, University Park, Pennsylvania, USA

[6]Department of Neurosurgery, Massachusetts General Hospital, Harvard Medical School, Boston, Massachusetts, USA

[7]Public Health Science, The Pennsylvania State University, University Park, Pennsylvania, USA

Correspondence Steven J. Greybush, Department of Meteorology and Atmospheric Science, The Pennsylvania State University, University Park, Pennsylvania, USA. sjg213@psu.edu.

†Deceased.

Yan Wang and Moussa Gueye are contributed equally.

Steven J. Greybush, Helen Greatrex, and Steven J. Schiff are contributed equally.

AUTHOR CONTRIBUTIONS

Yan Wang: Data curation (lead); formal analysis (lead); software (equal); visualization (equal); writing – original draft (supporting). **Moussa Gueye:** Data curation (equal); investigation (equal); software (supporting). **Steven J. Greybush:** Conceptualization (lead); data curation (equal); formal analysis (equal); investigation (lead); methodology (lead); resources (lead); software (lead); supervision (lead); validation (lead); visualization (lead); writing – original draft (lead); writing – review and editing (lead). **Helen Greatrex:** Conceptualization (lead); data curation (equal); formal analysis (supporting); investigation (lead); methodology (lead); supervision (equal); validation (lead); writing – original draft (lead); writing – review and editing (lead). **Andrew Whalen:** Investigation (supporting). **Paddy Ssentongo:** Investigation (supporting). **Fuqing Zhang:** Conceptualization (lead); investigation (equal); supervision (lead). **Gregory Jenkins:** Conceptualization (equal); investigation (equal); supervision (equal). **Steven J. Schiff:** Conceptualization (lead); funding acquisition (lead); investigation (lead); methodology (equal); project administration (lead); supervision (lead); writing – original draft (lead); writing – review and editing (lead).

CONFLICT OF INTEREST

The authors declare no conflicts of interest.

SUPPORTING INFORMATION

Additional supporting information can be found online in the Supporting Information section at the end of this article.

[8]Departments of Neurosurgery, Engineering Science and Mechanics, and Physics, The Pennsylvania State University, University Park, Pennsylvania, USA

[9]Department of Neurosurgery, Yale University, New Haven, Connecticut, USA

Abstract

Rainfall is an important variable to be able to monitor and forecast across Africa, due to its impact on agriculture, food security, climate-related diseases and public health. Numerical weather models (NWMs) are an important component of this work, due to their complete spatial coverage, high resolution and ability to forecast into the future. In this study, the spatio-temporal skill of short-term forecasts of rainfall across Africa from 2016 through 2018 is evaluated. Specifically, the European Centre for Medium-Range Weather Forecasts (ECMWF) and the National Centers for Environmental Prediction-Global Forecast System (NCEP-GFS) forecast models are verified by Rainfall Estimates 2.0 (RFE2) and African Rainfall Climatology Version 2 (ARC2), which are fused products of satellite and in situ observations and are commonly used in analysis of African rainfall. Model rainfall forecasts show good consistency with the satellite rainfall observations in spatial distribution over Africa on the seasonal timescale. Evaluation metrics of daily and weekly forecasts show high spatial and seasonal variations over the African continent, including a strong link to the location of the inter-tropical convergence zone (ITCZ) and topographically enhanced precipitation. The rainfall forecasts at 1 week aggregation time are improved against daily forecasts.

Keywords

Africa; ARC2; ECMWF; evaluation; GFS; model; rainfall; RFE2

1 | INTRODUCTION

1.1 | Motivation

Numerical weather prediction (NWP) provides tremendous societal benefit from the advanced warning of weather hazards to planning for economic activities such as agriculture (Alley et al., 2019). Improvements in in situ and remotely sensed observations, numerical model simulations, including their resolution and representation of physical processes, and the data assimilation techniques used to ingest these observations have led to the improved practical predictability of many weather phenomena (Houtekamer & Zhang, 2016). However, the availability of sufficient observations and regional models to forecast rainfall is limited in the African region, proving a challenge for NWP.

Operational numerical weather models (NWMs) are used to produce short-term and seasonal forecasts across the globe. In many countries, global NWP centers are well connected with their National Meteorological Agencies or Forecasting Offices, where forecasters are well trained and make best use of NWP products. The variations in skill of NWM across African geographies and climatologies are well studied (Gebremichael et al., 2022; Gebrechorkos et al., 2018; Kniffka et al., 2020; Linden et al., 2020; Maidment et al., 2013; Ogutu et al., 2017; Taraphdar et al., 2016; Tompkins & Feudale, 2010 among others). However, a large

proportion of research efforts have focused on seasonal or climate timescales, or restricted analysis to specific regions of Africa, or individual weather phenomena or events. Such studies are essential and provide high accuracy but are less helpful in understanding NWM performances comprehensively across the African continent as a whole. In addition, few studies have targeted the NWM performance of daily or weekly forecasts over a long time range, despite those having large societal impact (next section).

One of the reasons underpinning fewer large-scale assessments of NWM accuracy is that studies are often limited by the availability of ground-based observing networks for in situ verification of weather conditions, especially rainfall. While rain gauges provide relatively accurate and trusted measurements of precipitation at single points, their coverage is lacunar over many African regions. Remotely sensed rainfall products have been available since the early 1980s to fill this gap, supplementing a recent drop in available rain-gauge information (Washington & Downing, 1999).

1.2 | Implications for public health

Along with benefits for sectors such as agricultural monitoring and disaster risk management, the ability to better forecast short-term weather variables has especially important implications for public health (Heaney et al., 2016; Thomson et al., 2018; Thomson & Mason, 2019). Rainfall is vital to the dynamics of many infectious diseases. It also has a strong relationship with the seasonal variations of diseases in Africa such as seasonal Neisseria meningitis (Agier et al., 2017), malaria (Pascual et al., 2008), cholera (Koelle et al., 2005), or haemorrhagic fever (Bi et al., 1998).

The effect of rainfall on disease goes beyond seasonality, as short-term rainfall events can have a disproportionately large impact on disease outcomes. For example, Lemaitre et al. (2019) found that strong precipitation events modify the intra-seasonal double peak of epidemic cholera. Hand, foot and mouth disease (HFMD) also shows a complex association with weekly temperature and precipitation, with Hii et al. (2011) finding that in the Asia Pacific region weekly cumulative rainfall below 75 mm has a positive effect on transmission risk, while rain above 75 mm has a negative effect. When studying dengue, Hooshyar et al. (2020) showed that smaller rainfall peaks over March–April–May (MAM) could lead to larger case peaks over June–July–August (JJA). Equally, it has been found that heavy rainfall may quench and reduce dengue transmission, but dry spells in some settings could increase water storage in the environment, making it more suitable for breeding and propagation of the arthropod vectors that carry the disease (Fouque et al., 2006; Hii et al., 2011). Finally, and with relevance to the larger study this work is part of, bacterial infections leading to postinfectious hydrocephalus in East Africa appear to have a seasonal variation with rainfall (Paulson et al., 2020; Schiff et al., 2012), as does the bacterial disease melioidosis in Southeast Asia and Northern Australia (Wiersinga et al., 2018).

We suggest that high-quality forecasts of rainfall and other climate variables are a necessary and required component of what we term predictive personalized public health (P3H), where point-of-care decision-making can be improved through geospatial mapping that takes into account the functional relationships of the dynamics of infectious disease and environmental

factors. To do this, it is increasingly important to assess the short-term rainfall characteristics of available NWM models.

1.3 | Aim of this work

The aim of this study is to assess the performance in characterizing variations in precipitation of two operational NWMs, ECMWF and NCEP-GFS, across the continent of Africa. These were assessed at a continental scale for the years 2016–2018; a time frame selected both because these were years where contemporary NWP forecasts driven by modern observing systems were available across all products, and due to the relevance of 2016–2018 for a parallel public health predictive effort (Paulson et al., 2020). The predictive public health effort combines microbial surveillance with environmental factors (including remotely sensed and NWM rainfall) to improve point-of-care diagnostics and antimicrobial therapy for syndromes such as neonatal sepsis (Schiff et al., 2012) and to forecast epidemic disease (Ebeigbe et al., 2020; Ssentongo et al., 2021) in Africa.

Satellite rainfall estimates were selected as comparison datasets due to the uneven spatio-temporal distribution of ground-based weather networks across Africa. There are multiple satellite rainfall algorithms available, each with differing spatio-temporal skill; therefore, multiple datasets were selected to reduce dependence on individual product characteristics. Specifically, NOAA ARC2 and RFE2 were chosen for this study, with more details provided in Section 2.1.

In this article, Section 2 describes the NWM and satellite rainfall observation datasets, and Section 3 describes the methodology for validation. Because the importance of rainfall in public health applications goes beyond daily rainfall forecasts, this study assesses NWM forecast performance at daily, weekly and seasonal scales in Section 4. Finally, in Section 5, the implications for using these forecasts as inputs to public health prediction systems in the future are considered.

2 | DATA

2.1 | Observational dataset, NOAA RFE 2.0 and ARC 2.0

Satellite rainfall datasets are gridded and uniform in spatial coverage, with a high resolution and little missing data, proving advantageous for assessing NWM forecast accuracy. Across Africa, there are over 15 free, high-resolution products in operational use; from ‘single-sensor algorithms’, which typically use a combination of thermal infrared imagery and ground-based data to create homogeneous 30+ year rainfall records; to shorter time-series ‘multi-sensor’ algorithms, which also incorporate additional sensor input to allow additional rainfall features to be identified (Maidment et al., 2020). There is no perfect algorithm; products have varying skill depending on the seasonality, topography and geography of the area of interest (Awange et al., 2016; Tarnavsky & Bonifacio, 2020). Product selection also depends on the rainfall statistic of interest. For example, one product may more accurately capture severe rainfall but fail to properly capture long-term trends.

This study has therefore focused on two widely available products, cognizant that even as comparison datasets, they are likely to have biases. Specifically, this work uses NOAA

Rainfall Estimate Version 2 (RFE2) product and the NOAA Africa Rainfall Climatology Version 2 (ARC2). Both have a spatial resolution of 0.1 degrees and a daily temporal resolution.

As described in Xie and Arkin (1996), the Climate Prediction Center's NOAA RFE2 is available from January 2001, with an algorithm incorporating information from gauge data, geostationary infrared and polarorbiting microwave SSM/I and AMSU-B satellite data (Love et al., 2004; Novella & Thiaw, 2013). RFE2 has been shown to perform well across Africa (Thiemig et al., 2012), as well as in regional specific validations from Egypt (Abd Elhamid et al., 2020), Burkina Faso (Dembélé & Zwart, 2016), Ethiopia (Gebremicael et al., 2017), Mozambique (Toté et al., 2015), Sudan (Abd Elhamid et al., 2020) and Zimbabwe (Dinku et al., 2018). However, there is evidence to suggest that RFE2 captures rainfall less skillfully than several other products over East and Central Africa (Camberlin et al., 2019; Diem et al., 2014; Dinku et al., 2018; Nicholson & Klotter, 2021).

NOAA ARC2 is available from 1983 and is derived from a geographically static simple linear relationship between 'cold cloud duration' (the length of time a cloud is colder than a pre-defined threshold of 235 K) and historical rain-gauge amounts. This is then merged with rain-gauge data from the World Meteorological Organization's GTS network (Novella & Thiaw, 2013). ARC2 has a well-recorded bias in historical trend analysis (Cattani et al., 2020; Maidment et al., 2017) and has been shown to underperform other comparable satellite rainfall products such as CHIRPS or TAMSAT (Satgé et al., 2020; Tarnavsky & Bonifacio, 2020), especially in areas of complex terrain (Ayehu et al., 2018; Dinku et al., 2018). It shows better performance across West Africa (Dembélé & Zwart, 2016; Dembélé et al., 2020; Darko et al., 2021).

NOAA RFE2 and ARC2 were selected in part as comparison datasets due to their common use by end-users across weather risk management (Osgood & Shirley, 2012), disease modelling (Mbouna et al., 2019; Fall et al., 2022; Kim et al., 2019; Ngwa et al., 2016; Ssentongo et al., 2018) and Personalized Predictive Health (Agamile & Lawson, 2021), who might also have interest in the ability of forecasts to 'sync' with these estimates. The choice also allows the results of this work to be directly compared with several other forecast validation efforts over Africa. For example, RFE2 forms one of the validation datasets for TIGGE forecasts in Louve et al. (2016) and ARC2 in efforts such as Ogutu et al. (2017). However, an important next step in this effort will be to incorporate additional skillful observational products across Africa such as University of California Santa Barbara's Climate Hazard's group Infrared Precipitation with Stations (CHIRPS), University of Reading's TAMSAT, and NASA's Integrated Multi-satellitE Retrievals (IMERG).

In this study, RFE2 and ARC2 gridded satellite rainfall estimates are used as the observation data to verify the NWM predictions. The main results of NWM forecasts against the RFE2 rainfall are shown in the main article figures, while the results against the ARC2 are shown in the supplemental figures. Further information about the datasets is shown in Table 1.

2.2 | NWM forecasts

The ECMWF and NCEP-GFS are two of the most common products used in global and regional weather and climate forecasting, hydrology, public health and other applications (Elless & Torn, 2019; Karrouk, 2019; Kerns & Chen, 2014; Meynadier et al., 2010; Nikulin et al., 2012; Sajadi et al., 2020).

The ECMWF's Integrated Forecasting System is used to predict weather and climate using a high-resolution (9 km) global model and data assimilation system and has demonstrated considerable skill for synoptic-scale variables in the medium-range in the mid-latitudes (Buizza & Leutbecher, 2015; Park et al., 2008). At the National Centers for Environmental Prediction, the GFS, initialized with the Global Data Assimilation System, creates 16-day predictions four times daily, and output from this model is made available freely around the world. Both data assimilation systems ingest millions of observations from satellite, airborne, ground-based, and ocean-based observing platforms to provide initial conditions for the modelling systems (Cucurull et al., 2007; Kleist et al., 2009), and atmospheric conditions are projected forward in time using the set of equations encoded in the model's dynamical core and physical parameterization schemes. Both the ECMWF and GFS forecasts used in this study are initialized at 12:00 UTC (Table 1). Previous studies have reported that the NCEP-GFS has an advantage over the ocean regions, while the ECMWF products are more reasonable over the Northern Hemisphere continents (Bosilovich et al., 2008; Taraphdar et al., 2016). This study further explores their performances over the African continent.

3 | METHODS

3.1 | Verification scale

At 0.1 degrees, the RFE2 and ARC2 satellite rainfall products have finer spatial resolution than GFS or ECMWF. In order to better compare the rainfall products and forecasts, the satellite observations were rescaled to the model spatial grid of 0.5 degrees. Meanwhile, the temporal resolutions of NWM forecasts are 6 h, finer than the rainfall estimates of daily resolution, thus the NWM forecast rainfall were summed to a daily timescale. At the daily aggregation scale, 1-day lead time NWM forecasts (daily forecast sum) were compared with daily resolution satellite observations valid for the same time period (i.e., the days for which the forecasts were predicted match the days the rainfall was observed). At the weekly aggregation scale, NWM forecasts for days 1–7 (at lead times of 1–7 days) were summed together, and this 1-week cumulative prediction estimate was compared against the observed 1-week cumulative rainfall estimate valid for the same time period. Weekly forecasts were assessed for each range of dates in the dataset (e.g., days 1–7, 2–8, 3–9, etc.).

3.2 | Verification metrics

Several widely used statistical scores were applied to evaluate the NWM forecast performance against the satellite observations, including subtractive bias, root mean squared error (RMSE), Pearson's correlation coefficient (r), accuracy (A), threat score (TS), probability of detection (POD), false alarm ratio (FAR), and Brier score (BS). These are summarized further below and in Table 2.

The skill of ECMWF and GFS forecast rainfall in these metrics was compared against the RFE2 and ARC2 satellite rainfall estimates. The correlation coefficient r was applied to measure the strength of the linear relationship between the NWM forecasts and satellite observations. The significance of this result was assessed using a p-value, following a Student's t-distribution test, representing the probability that r between the forecast and observations occurred by chance. In this study, r is treated as significant when the effective day number (defined as the number of days when there are no missing values in both NWM and satellite data) is larger than 20 and the absolute p-value is less than 0.01; in other words, when a positive correlation between model forecast and satellite observation is of sufficient magnitude to be judged as skillful.

Dichotomous metrics were used to evaluate binary (yes/no) forecasts of rainfall that exceed a threshold amount. It is important to note that there is a complex relationship between NWM forecast error and the values of dichotomous metrics, in part due to the inherent loss of information when dichotomizing a continuous variable such as rainfall (Tartaglione, 2010). Acknowledging this, these commonly used metrics were included to allow intercomparison between other NWM forecast and precipitation validation studies (for example, Kidd et al., 2012; McBride & Ebert, 2000; Pennelly et al., 2014) and to provide some insight into the ability of the models to capture rain/no rain. Accordingly, a daily threshold of 2 mm was applied to denote the difference between rain and no rain. This is a commonly used threshold used in rain/no rain impact modelling across sub-Saharan Africa chosen as rainfall amounts less than 2 mm are likely to evaporate rather than be regarded as 'useful' rain (Bennett et al., 2011; Mupangwa et al., 2011).

Specific event-based statistics applied include the dichotomous-accuracy, A, which is simply the fraction of satellite observed events (either rain or dry) 'correctly forecast' in NWM predictions. By correctly forecast, we mean that they correspond with the relevant satellite rainfall estimate rather than against a 'perfect' rainfall observation. The TS represents a somewhat more balanced score of NWM forecast predictions as it removes the cases when no rain was forecast, and no rain was observed (which in some regions represents a majority of cases). The FAR explains the fraction of NWM forecast events that did not occur in the relevant satellite products. The POD compares true positives to all days when rain was observed in the satellite product. Finally, the BS was used to indicate the magnitude of probability forecast errors.

3.3 | Regions of interest

In order to more clearly understand spatial differences in NWM forecast performance over Africa, validation metrics were calculated separately over Northern Africa (NA, land: 19°W-40° E, 20°N-36°N), Western Africa (WA, land: 19° W–10° E, 0° N–20° N), Eastern Africa (EA, land: 30° E–51° E, 10° S–20° N), Central Africa (CA, land: 10° E–40° E, 10° S–20° N) and Southern Africa (SA, land: 10° E–40° E, 36° S–10° S), as indicated in Figure 1. All evaluations are performed over the African landmass, while the ocean is masked.

4 | RESULTS

4.1 | Spatial and seasonal pattern

African annual rainfall shows considerable spatial variation, with the largest climatological values of precipitation concentrated around the equatorial region and dominated by the Intertropical Convergence Zone, ITCZ (Figure 1). Figure 2 depicts the spatial pattern of averaged daily rainfall, broken down by season and product. The NWM rainfall forecasts from both ECMWF and GFS show a similar overall spatial pattern over Africa for each season, which are similar to those patterns observed by satellite. For example, the general seasonality of the rainfall belt, controlled by the movement of the ITCZ, is captured in its north–south movement by all four products. The differences between west coastal and east coastal Africa also are clearly represented in the NWM forecasts, especially during December–January–February (DJF) and June–July–August (JJA) (Figure 2, columns 1 and 3). It is interesting to note that terrain-enhanced rainfall is more pronounced in GFS compared with ECMWF. For example, Ethiopia's Bale Mountain range (40 E 8 N) in MAM and JJA, and the Marra Mountain range in western Sudan (34 E 13 N) in JJA are clearly visible in the model output.

4.2 | Verification of NWM forecasts at daily scale

Overall, both NWM and the satellite observations show a similar overall magnitude of rainfall amounts. For example, the spatial mean of total rainfall in 3 years from 2016 to 2018 across the whole Africa continent, is very similar across both satellites (ARC2: 1718 mm, RFE2: 1772 mm) and models (ECMWF: 1786 mm, GFS: 1714 mm). Despite this, there are clear spatial differences between the NWP forecasts and satellite observations at daily timescales. For example, both the ECMWF and GFS forecasts tend to underestimate rainfall totals in tropical Africa while overestimating rainfall totals elsewhere (Figure 3 and Figure S1). The largest (subtractive) bias occurs over and around the ITCZ rainfall region; both ECMWF and GFS tend to have larger biases over West Africa than that in other regions, especially during JJA. The Central and East African highlands are another important region of precipitation bias, shown especially in the GFS forecast.

As shown in Figure 3, ECMWF and GFS differ in their spatial representation of African rainfall, especially over the coastal regions of West Africa. One of the most significant differences is in the placement of the ITCZ during JJA; there is a strong dry bias in the GFS at around 10 N, while the bias is somewhat weaker and placed further north in the ECMWF, with a wet bias appearing around 5 N. A spatial pattern such as this is often observed when two datasets disagree on either the speed or spatial extent of the ICTZ movement, for example, in this case, it appears that both models underestimate the Northern extent of timing of the West African monsoon. This corresponds with previous research on both the ECMWF family of products (ECMWF System 3: Tompkins & Feudale, 2010) and the GFS family of products (Xue et al., 2010), which found NWMs have a tendency to displace the rainfall in the West African Monsoon too far south. These discrepancies might be partially attributable to errors in convective parameterization schemes. This conclusion is also supported by the fact that convection systems contribute more than 50% of the annual rainfall over the west coast equatorial region (Maranan et al., 2018), but are difficult to

predict well without a convection-allowing (grid spacing 3 km or smaller) model (e.g., Clark et al., 2016).

Our results also indicate that complex topography and terrain make an important contribution to the NWM forecast bias. Terrain is conducive to generating lift, and therefore triggering convection (as evidenced by enhanced rainfall over terrain in East Africa and Madagascar). The GFS is also more sensitive to topographically enhanced precipitation, showing a wet bias relative to satellite estimates. Additionally, biased water vapour measurements and sparsity of available observational data are likely contributing factors to the forecast biases, as poor initial conditions lead to deficiencies in model depictions of rainfall (Jiang et al., 2015). It is likely that these measurement quality factors could also contribute to the different performances among different NWMs.

When considering RMSE at the daily scale, the timing of precipitation becomes more important rather than just the seasonal totals used to calculate the bias. In Figure 4 and Figure S2, higher values of RMSE were centred on the ITCZ rainfall regions during each season. The GFS model has larger RMSE values than the ECMWF, especially over the ITCZ rainfall regions. While the models have identified the general region and seasonality of the ITCZ, it is especially challenging to predict the exact day, location and amount of rainfall from local convection. Large-scale NWM forecast rainfall spatial patterns are controlled by local circulation patterns, such as Land-Based Convergence Zones, which are closely connected with the tropical Atlantic ITCZ in the ECMWF model but more dominated by Indian Ocean ITCZ in the GFS model (Zhang et al., 2013). The degree to which the models correctly depict the amplitude and phase of African Easterly Waves would also be reflected in the RMSE.

As described in the methods, the correlation coefficient (r) was used to determine the degree of linear association between NWM forecasts and satellite observations across the temporal dimension. Figures 5 and S3 show spatial distributions of correlation coefficient at locations with positive skill (p-value less than 0.01 and effective day number of 20). These criteria were set to avoid spurious linear correlation values caused by missing information or very high percentage of dry days, especially over North Africa where the NWM forecasts have a very large correlation coefficient but do not reach statistical significance at most locations. The greatest model skill at the daily timescale is found from 0 to 10 N in DJF, and 10–20 S and over East Africa in MAM and SON. In many regions, the NWM forecasts cannot explain the observed rainfall well at the daily scale. This is especially apparent during JJA, as less than 10% of the locations in either forecast have substantial linear correlation with the RFE2 rainfall (Figure 5c,g). Furthermore, at each location, less than 50% variation of the observed rainfall could be explained by the NWM forecasts. During March–April–May (MAM), the correlation coefficient in the SA region is larger than that of other seasons, while in September–October–November (SON), the correlation in the West Africa region is stronger than other seasons. In addition, the ECMWF forecasts show a stronger correlation with the satellite estimates than the GFS during all four seasons (Figures 5 and S3). The correlation coefficients show an interesting spatial pattern, which does not appear to be fully linked with the progression of the ITCZ. A band of higher correlation coefficients is seen across West Africa during the dry season, but an equivalent band is not seen in the

Southern Hemisphere. Very low correlation coefficients are also seen in Western Equatorial Africa, a region dominated by limited observing networks and a complex synoptic situation (Nicholson, 2013), suggesting that NWMs are less able to capture the dynamics in that region. While examining correlations across three-month periods removes much of the role of seasonality (rather than sub-seasonal, weekly and daily variability) contributing to correlations, some of the correlation from the seasonal cycle may still be included due to monthly shifts in rainfall climatology.

We now turn to dichotomous (hit/miss) statistics to assess the ability of the NWM forecasts to capture the occurrence of rainfall events. The results for ECMWF are depicted in Figure 6, with the results for GFS shown in Figure 7. Overall, many of the dichotomous metrics were dominated by the large-scale climatology of the study area, in part due to the nature of the statistics themselves. For example, for both models, high dichotomous-accuracies, A, were recorded in climatologically dry regions, or perpetually dry areas such as the Sahara Desert (Figures 6 and 7a–d). TS (Figures 6 and 7e–h) is a metric that excludes the case of both model and observation having no precipitation, which is more appropriate for these areas. In comparison, the general drop in accuracy in rainy season areas is due to the fact that during the rainy season ‘a rain day’ is less dominant in a climatological category than a dry day is in the dry season. For example, there are often days during the rainfall season when it does not rain, but typically very few rain days in the dry season. As the accuracy is therefore heavily influenced by the most common climatological category (rain/no rain), it is included here as the lowest bar a dichotomous forecast should pass and suggest that the result provides additional confirmation that in general the model is reproducing the large-scale movement of the ICTZ.

At the next level of complexity, the POD depicted in Figures 6 and 7i–l, and the FAR, depicted in Figures 6 and 7m–p, are studied. For these statistics, a value of 1 means a high POD (good) or a high FAR (bad). In general, these also capture the movement of the ICTZ, although there is evidence that ECMWF is capturing orographic rainfall increases in areas such as the western Ethiopian highlands (JJA and SON). This result has been independently confirmed across several other studies and forecast timescales (for example Ehsan et al. (2021) at seasonal timescales). It is also worth noting that this is a complex region where satellite rainfall datasets can also struggle to accurately capture rainfall occurrences (Dinku et al., 2007). Subtle differences are also seen between ECMWF and GFS, for example, in South Africa during JJA, GFS captures a different pattern of rainfall events than ECMWF, with ECMWF forecasting broadly more rainfall in the region, leading to more captured rainfall events at the expense of higher false alarms. In general, higher false alarm ratios are seen at the edges of the ICTZ rainfall band, adding further evidence that the models might be mischaracterizing the exact location of the ITCZ in a given year. This is likely to be highlighted given the relatively short time period used in the analysis (2016–2018). The short time period and low threshold for rain/no rain also means that some data artefacts are apparent, for example, the small area of higher POD in Nigeria in the DJF ‘dry season’ is likely due to a single rainfall event.

Finally, the TS is shown in Figures 6 and 7e–h and the BS is shown in Figures 6 and 7q–t. The TS measures the proportion of correctly predicted forecast events, for example,

the accuracy when correct negatives have been removed, while the BS, or frequency bias, assesses the magnitude of the probability of forecast errors. Both confirm similar spatial patterns to those discussed above, although it is interesting to note the higher skill in East Africa during the early rains (MAM). In general at a daily scale, our results are consistent with several previous regional studies including Kniffka et al. (2020), Camberlin et al. (2019), Vogel et al. (2018), Parker and Diop-Kane (2017) and Ma et al. (2019), which show limited daily model skill. We therefore suggest that although the daily forecasts are able to capture large-scale features, if one is interested in precision for the rainfall occurrence at a specific 0.5 degree pixel on a specific day, both ECMWF and GFS still have room for improvement.

It is worth highlighting that through the lens of public health or other applications, even when models struggle to forecast daily pixel-scale rainfall, higher skill is often observed for other convective statistics that could prove useful predictors of public health. For example, Vigaud and Giannini (2019) recorded higher categorical skill scores when assessing the ability of ECMWF forecasts to correctly classify a location into one of seven convective regimes. It should also be noted that the daily dichotomous skill scores in Figures 6 and 7 for rainfall might be depressed due to diurnal reporting mismatch. Both NWM and satellite rainfall observations are poor at predicting the exact hour rainfall occurred (Greatrex et al., 2014). Therefore, given that tropical convective rainfall often falls overnight, it is common to observe a 1-day mismatch in daily rainfall records where one rainfall event is split over 2 days in one product, but recorded in a single day in another. Equally, cloud features such as cirrus anvils can also lead to reduced satellite rainfall skill at a daily scale compared with temporally aggregated data, and the binary nature of dichotomous hit/miss statistics mean that these mismatches are heavily penalized. In the next section, we therefore consider weekly scale verification to remove these biases.

4.3 | Weekly scale verification and influence of forecast lead time

As the skill of an NWM forecast is highly dependent on verification timescale, NMW forecasts of aggregated rainfall over 1 week were assessed and compared with daily rainfall forecasts with a lead time of 1 day (Figures 3–9). Precipitation biases at a weekly scale were reduced from the 1-day forecasts (Figure 3), reflecting the impact of model initialization and forecast spin-up in developing convective systems. At a weekly timescale, both the ECMWF and GFS forecasts show better performances than those at a daily timescale, a primary reason for this being the cancellation of random errors during the aggregation process. For example, weekly forecasts show lower RMSE (Figure 4) and higher correlation coefficients (Figure 5). The improvements in RMSE were especially prevalent over areas dominated by the ITCZ; the more frequent the rainfall events, the more likely that aggregating to a 1-week timescale improves performance. For correlation coefficient, the largest improvements were at the edges of areas of rainfall; north of the equator in DJF, in SA and East Africa in MAM and SON; skill remained low in JJA. Differences in dichotomous statistics for the ECMWF (Figure 8) and the GFS (Figure 9) share a similar spatial pattern. Improvements in accuracy followed the seasonal movement of the ITCZ; regions in their rainy season often exceeded the threshold precipitation value for weekly precipitation in both model and observations, making this an easier forecast than at the daily scale where this may not happen every day at

a particular location. Likewise, TS and POD also improved over those regions (particularly Central and SA). For FAR, improvements were more modest and did not reveal a clear spatial pattern. For BS, improvements (reductions in score) also followed the ITCZ and regions of improved accuracy.

NWM performance also depends on forecast lead time (e.g., Greybush et al., 2017). While the models capture seasonal changes in rainfall, it is difficult to predict weather and climate anomalies at long lead times of weeks or months due to the chaotic nature of the atmosphere (Luo & Wood, 2006). At shorter sub-daily time ranges, NWM forecasts would need to capture the location of convection elements, or individual thunderstorm clusters. Therefore, the differences between NWM and satellite datasets would increase when they are evaluated on a finer timescale or at a longer lead time. For rainfall, it appears the benefit of aggregating rainfall over a 7-day period outweighs forecast degradation at lead times extending from 1 to 7 days.

The results suggest that as indicated in the previous section, improvements in model skill might be achieved through less emphasis on the exact time of an individual rainfall event. This has important implications for end-user applications, especially in agriculture and health, as the majority of such uses are not reliant on knowing the precise rainfall at a specific time on a specific day but rather the cumulative impacts of an excess or deficit of rainfall. We suggest that 1-week aggregated NMW forecasts show potential in supporting public health and other end-user needs.

4.4 | Differences in rainfall intensity and frequency between forecast and satellite

Rainfall intensity and frequency are key factors of the temporal and spatial variations shown in previous figures. Therefore, Figure 10 compares the relative distribution of events (cumulative number of days over all locations) falling in each of six daily precipitation intensity categories between RFE2 and ECMWF, separated by season. The lowest intensity events (less than 2 mm day^{-1}, which count as no rain for the dichotomous statistics) comprise the greatest number of days, with more such days in JJA and SON for the ECMWF compared with RFE2 in MAM, JJA and SON. This pattern flips for events of 2–10 mm day^{-1}, with RFE2 having more such events in all seasons compared with ECMWF. As the rainfall threshold increases, events become less common. For rainfall of more than 20 mm day^{-1}, there are clearly many more model-predicted events than observed events. This figure shows that there are more low-intensity (less than 2 mm day^{-1}) and high-intensity (>20 mm day^{-1}) rainfall events forecasted by the NWM than observed, which has importance if the forecasting application depends upon the amount of rainfall. Figures S4–S8 repeat the analysis of Figure 10 for the five regions of Africa defined in Figure 1.

5 | DISCUSSION AND CONCLUSIONS

This study examined the skill of NWM forecasts relative to satellite rainfall observations over Africa during 3 years: 2016–2018. It was shown that two NWM forecasts, ECMWF and GFS, show large spatial and seasonal variabilities in skill over the African continent. In terms of seasonal climatology, the NWMs generally reproduced observed amounts and locations, with some discrepancies in location of the ITCZ and amount of orographic

precipitation. On the shorter timescale, ECMWF forecasts demonstrated better performance than GFS forecasts in terms of lower RMSE and FAR values and higher accuracy and correlation coefficient. As expected, a weekly aggregation time compared with a daily aggregation time exhibited higher correlation, TS and POD, as well as lower RMSE values. These results show that NWM forecasts do have some positive skill relative to satellite observations, but that there is substantial room for improvements in precipitation forecasting. This could be obtained via better observations, data assimilation techniques, and model resolution and parameterizations (such as convection parameterizations). Model skill over Africa is lower than in other parts of the world with more dense observing systems, such as North America (Yang et al., 2017). In addition, the use of regional high-resolution, convection-allowing models (with grid spacings of 3 km or less) may better resolve local mesoscale weather phenomena, such as lake breeze convection, orographic convection, the diurnal cycle of convection and other mesoscale convective systems, leading to improvement in the predictive skill of precipitation.

Potential limitations arise from the focus constraint on the years 2016–2018. This three-year period may exclude certain extreme weather and climate events that could have led to different quantitative metrics of prediction skill. They also mean that especially in the dry season areas, some validation features might be the result of very few rainfall events. The advantage of using this time period is its relative recency, allowing us to only validate modern NWM forecasts, observations and assimilation systems, as well as alignment with the needs of ongoing public health projects. Considering these advantages and limitations, we expect the broad conclusions of this article to be applicable to other years not included in the study.

It is also important to note that the results of this study could be impacted by our choice of satellite comparison datasets, NOAA RFE2 and NOAA ARC2. This is especially important, as discussed in Section 2.1 both products have shown systematic bias and limited skill in several regions of Africa. An important next step will be to repeat the results of this work with a variety of other satellite products.

The results of this study have important implications for public health P3H efforts. Many infectious diseases, such as cholera, dengue and malaria, are all influenced by meteorological factors (Koelle et al., 2005). During the COVID-19 pandemic, African meteorological variables, especially humidity and temperature, have been shown to influence the predictability of cases (Ssentongo et al., 2021). There is increasing evidence that certain soil bacteria, such as the Burkholderia that causes melioidosis in Southeast Asia and Northern Australia (Wiersinga et al., 2018), and perhaps the Paenibacillus that causes infant brain infections and postinfectious hydrocephalus in East Africa (Paulson et al., 2020; Schiff et al., 2012), may be environmentally influenced by rainfall. If soil moisture is important in regulating the infectivity of soil and drinking water, then fusing public health microbial surveillance with satellite environmental measurements and NWM forecasts forms a natural combination. Such fusion offers the prospect of real-time prediction of the likely organisms infecting patients who present with signs and symptoms of serious bacterial infections. Causative organism prediction is critical in the proper selection of antibiotics. In low- and middle-income countries, where availability of microbiological laboratory testing

is limited, predictive methods may offer immediacy in guiding antimicrobial treatment alternatives. Furthermore, P3H efforts fusing historical microbial surveillance patterns with environmental factors can be utilized in optimized prevention efforts focusing attention on places and timing where the anticipated infection risk is greatest. Finally, bacteria in soil, or arthropod vectors breeding in water, require relevant timescales to increase their density. Such timescales are typically longer than individual days, and likely extend to one or more weeks. Therefore, our demonstration in this present study of increased forecasting skill utilizing 1-week cumulative rainfall is of particular interest in further exploration of P3H.

Supplementary Material

Refer to Web version on PubMed Central for supplementary material.

ACKNOWLEDGEMENTS

We dedicate this work to the memory of Professor Fuqing Zhang, our colleague who was vital to the concept and initiation of this project.

Funding information

National Institute of Allergy and Infectious Diseases, Grant/Award Number: R01AI145057

This work was supported by an NIH Director's Transformative Award 1R01AI145057.

DATA AVAILABILITY STATEMENT

GFS and ECMWF NWM data are available for download at the UCAR (https://rda.ucar.edu/datasets/ds084.1/) and TIGGE (http://apps.ecmwf.int/datasets/data/tigge/levtype=sfc/type=cf/) websites, respectively. RFE2 (ftp://ftp.cpc.ncep.noaa.gov/fews/fewsdata/africa/rfe2/) and ARC2 (ftp://ftp.cpc.ncep.noaa.gov/fews/fewsdata/africa/arc2/) datasets are available from the NOAA NCEP Climate Prediction Center website.

REFERENCES

Abd Elhamid AMI, Eltahan AMH, Mohamed LME & Hamouda IA (2020) Assessment of the two satellite-based precipitation products TRMM and RFE rainfall records using ground based measurements. Alexandria Engineering Journal, 59(2), 1049–1058. Available from: 10.1016/j.aej.2020.03.035

Agamile P & Lawson D (2021) Rainfall shocks and children's school attendance: evidence from Uganda. Oxford Development Studies, 49(3), 291–309.

Agier L, Martiny N, Thiongane O, Mueller JE, Paireau J, Watkins ER et al. (2017) Towards understanding the epidemiology of Neisseria meningitidis in the African meningitis belt: a multi-disciplinary overview. International Journal of Infectious Diseases, 54, 103–112. Available from: 10.1016/j.ijid.2016.10.032 [PubMed: 27826113]

Alley RB, Emanuel KA & Zhang F (2019) Advances in weather prediction. Science, 363(6425), 342–344. Available from: 10.1126/science.aav7274 [PubMed: 30679358]

Awange JL, Ferreira VG, Forootan E, Khandu, Andam-Akorful SA, Agutu NO. et al. (2016) Uncertainties in remotely sensed precipitation data over Africa. International Journal of Climatology, 36(1), 303–323. Available from: 10.1002/joc.4346

Ayehu GT, Tadesse T, Gessesse B & Dinku T (2018) Validation of new satellite rainfall products over the Upper Blue Nile Basin, Ethiopia. Atmospheric Measurement Techniques, 11(4), 1921–1936. Available from: 10.5194/amt-11-1921-2018

Bennett JC, Diggle A, Evans F & Renton M (2011) Towards measures of the eradicability of rain-splashed crop diseases. In: Chan F, Marinova D & Anderssen RS (Eds.) MODSIM2011, 19th international congress on modelling and simulation. 19th international congress on modelling and simulation. New Zealand: Modelling and Simulation Society of Australia and New Zealand Inc. Available from: 10.36334/modsim.2011.E16.bennett

Bi P, Wu X, Zhang F, Parton KA & Tong S (1998) Seasonal rainfall variability, the incidence of hemorrhagic fever with renal syndrome, and prediction of the disease in low-lying areas of China. American Journal of Epidemiology, 148(3), 276–281. Available from: 10.1093/oxfordjournals.aje.a009636 [PubMed: 9690365]

Bosilovich MG, Chen J, Robertson FR & Adler RF (2008) Evaluation of global precipitation in reanalyses. Journal of Applied Meteorology and Climatology, 47(9), 2279–2299. Available from: 10.1175/2008JAMC1921.1

Buizza R & Leutbecher M (2015) The forecast skill horizon. Quarterly Journal of the Royal Meteorological Society, 141(693), 3366–3382. Available from: 10.1002/qj.2619

Camberlin P, Barraud G, Bigot S, Dewitte O, Makanzu Imwangana F, Maki Mateso JC et al. (2019) Evaluation of remotely sensed rainfall products over Central Africa. Quarterly Journal of the Royal Meteorological Society, 145(722), 2115–2138.

Cattani E, Merino A & Levizzani V (2020) Rainfall trends in East Africa from an ensemble of IR-based satellite products. In: Levizzani V, Kidd C, Kirschbaum DB, Kummerow CD, Nakamura K & Turk FJ (Eds.) Satellite precipitation measurement, Vol. 2. Switzerland: Springer International Publishing, pp. 791–817. Available from: 10.1007/978-3-030-35798-6_17

Clark P, Roberts N, Lean H, Ballard SP & Charlton-Perez C (2016) Convection-permitting models: a step-change in rainfall forecasting. Meteorological Applications, 23(2), 165–181.

Cucurull L, Derber JC, Treadon R & Purser RJ (2007) Assimilation of global positioning system radio occultation observations into NCEP's global data assimilation system. Monthly Weather Review, 135(9), 3174–3193. Available from: 10.1175/MWR3461.1

Darko S, Adjei KA, Gyamfi C, Odai SN & Osei-Wusuansa H (2021) Evaluation of RFE satellite precipitation and its use in streamflow simulation in poorly gauged basins. Environmental Processes, 8(2), 691–712.

Dembélé M, Schaefli B, van de Giesen N & Mariéthoz G (2020) Suitability of 17 gridded rainfall and temperature datasets for large-scale hydrological modelling in West Africa. Hydrology and Earth System Sciences, 24, 5379–5406. Available from: 10.5194/hess-24-5379-2020

Dembélé M & Zwart SJ (2016) Evaluation and comparison of satellite-based rainfall products in Burkina Faso, West Africa. International Journal of Remote Sensing, 37(17), 3995–4014. Available from: 10.1080/01431161.2016.1207258

Diem JE, Hartter J, Ryan SJ & Palace MW (2014) Validation of satellite rainfall products for western Uganda. Journal of Hydrometeorology, 15(5), 2030–2038.

Dinku T, Ceccato P, Grover-Kopec E, Lemma M, Connor SJ & Ropelewski CF (2007) Validation of satellite rainfall products over East Africa's complex topography. International Journal of Remote Sensing, 28(7), 1503–1526.

Dinku T, Funk C, Peterson P, Maidment R, Tadesse T, Gadain H et al. (2018) Validation of the CHIRPS satellite rainfall estimates over eastern Africa. Quarterly Journal of the Royal Meteorological Society, 144(S1), 292–312. Available from: 10.1002/qj.3244

Ebeigbe D, Berry T, Schiff SJ & Sauer T (2020) Poisson Kalman filter for disease surveillance. Physical Review Research, 2(4), 043028. Available from: 10.1103/PhysRevResearch.2.043028 [PubMed: 39211287]

Ehsan MA, Tippett MK, Robertson AW, Almazroui M, Ismail M, Dinku T et al. (2021) Seasonal predictability of Ethiopian Kiremt rainfall and forecast skill of ECMWF's SEAS5 model. Climate Dynamics, 57(11), 3075–3091.

Elless TJ & Torn RD (2019) Investigating the factors that contribute to African easterly wave intensity forecast uncertainty in the ECMWF ensemble prediction system. Monthly Weather Review, 147(5), 1679–1698. Available from: 10.1175/MWR-D-18-0071.1

Fall P, Diouf I, Deme A & Sene D (2022) Assessment of climate-driven variations in malaria transmission in Senegal using the VECTRI model. Atmosphere, 13(3), 418.

Fouque F, Carinci R, Gaborit P, Issaly J, Bicout DJ & Sabatier P (2006) Aedes aegypti survival and dengue transmission patterns in French Guiana. Journal of Vector Ecology, 31(2), 390–399. [PubMed: 17249358]

Gebrechorkos SH, Hülsmann S & Bernhofer C (2018) Evaluation of multiple climate data sources for managing environmental resources in East Africa. Hydrology and Earth System Sciences, 22(8), 4547–4564. Available from: 10.5194/hess-22-4547-2018

Gebremicael TG, Mohamed YA, van der Zaag P, Berhe AG, Haile GG, Hagos EY et al. (2017) Comparison and validation of eight satellite rainfall products over the rugged topography of Tekeze-Atbara Basin at different spatial and temporal scales. Hydrology and Earth System Sciences Discussions, 1–31. Available from: 10.5194/hess-2017-504

Gebremichael M, Yue H & Nourani V (2022) The accuracy of precipitation forecasts at timescales of 1–15 days in the Volta River Basin. Remote Sensing, 14(4), 937.

Greatrex H, Grimes D & Wheeler T (2014) Advances in the stochastic modeling of satellite-derived rainfall estimates using a sparse calibration dataset. Journal of Hydrometeorology, 15(5), 1810–1831.

Greybush SJ, Saslo S & Grumm R (2017) Assessing the ensemble predictability of precipitation forecasts for the January 2015 and 2016 East Coast Winter storms. Wea. Forecasting, 32, 1057–1078. Available from: 10.1175/WAF-D-16-0153.1

Heaney A, Little E, Ng S & Shaman J (2016) Meteorological variability and infectious disease in Central Africa: a review of meteorological data quality: meteorology and infectious disease in C. Africa. Annals of the New York Academy of Sciences, 1382(1), 31–43. Available from: 10.1111/nyas.13090 [PubMed: 27244461]

Hii YL, Rocklöv J & Ng N (2011) Short term effects of weather on hand, foot and mouth disease. PLoS One, 6(2), e16796. Available from: 10.1371/journal.pone.0016796 [PubMed: 21347303]

Hooshyar M, Wagner CE, Baker RE, Metcalf CJE, Grenfell BT & Porporato A (2020) Cyclic epidemics and extreme outbreaks induced by hydro-climatic variability and memory. Journal of the Royal Society Interface, 17(171), 20200521. [PubMed: 33081643]

Houtekamer PL & Zhang F (2016) Review of the ensemble Kalman filter for atmospheric data assimilation. Monthly Weather Review, 144(12), 4489–4532. Available from: 10.1175/MWR-D-15-0440.1

Jiang JH, Su H, Zhai C, Wu L, Minschwaner K, Molod AM et al. (2015) An assessment of upper troposphere and lower stratosphere water vapor in MERRA, MERRA2, and ECMWF reanalyses using Aura MLS observations. Journal of Geophysical Research: Atmospheres, 120(22), 11–468.

Karrouk M-S (2019) The shift of the atmospheric circulation patterns and its impacts on Western Mediterranean. In: Zhang Z, Khélifi N, Mezghani A & Heggy E (Eds.) Patterns and mechanisms of climate, paleoclimate and Paleoenvironmental changes from low-latitude regions. Switzerland: Springer International Publishing, pp. 107–110.

Kerns BW & Chen SS (2014) ECMWF and GFS model forecast verification during DYNAMO: multiscale variability in MJO initiation over the equatorial Indian Ocean. Journal of Geophysical Research: Atmospheres, 119(7), 3736–3755. Available from: 10.1002/2013JD020833

Kidd C, Bauer P, Turk J, Huffman GJ, Joyce R, Hsu KL et al. (2012) Intercomparison of high-resolution precipitation products over Northwest Europe. Journal of Hydrometeorology, 13(1), 67–83.

Kim Y, Ratnam JV, Doi T, Morioka Y, Behera S, Tsuzuki A et al. (2019) Malaria predictions based on seasonal climate forecasts in South Africa: a time series distributed lag nonlinear model. Scientific Reports, 9(1), 17882. Available from: 10.1038/s41598-019-53838-3 [PubMed: 31784563]

Kleist DT, Parrish DF, Derber JC, Treadon R, Wu W-S & Lord S (2009) Introduction of the GSI into the NCEP global data assimilation system. Weather and Forecasting, 24(6), 1691–1705. Available from: 10.1175/2009WAF2222201.1

Kniffka A, Knippertz P, Fink AH, Benedetti A, Brooks ME, Hill PG et al. (2020) An evaluation of operational and research weather forecasts for southern West Africa using observations from the DACCIWA field campaign in June–July 2016. Quarterly Journal of the Royal Meteorological Society, 146(728), 1121–1148. Available from: 10.1002/qj.3729

Koelle K, Rodó X, Pascual M, Yunus M & Mostafa G (2005) Refractory periods and climate forcing in cholera dynamics. Nature, 436(7051), 696–700. Available from: 10.1038/nature03820 [PubMed: 16079845]

Lemaitre J, Pasetto D, Perez-Saez J, Sciarra C, Wamala JF & Rinaldo A (2019) Rainfall as a driver of epidemic cholera: comparative model assessments of the effect of intra-seasonal precipitation events. Acta Tropica, 190, 235–243. Available from: 10.1016/j.actatropica.2018.11.013 [PubMed: 30465744]

Levy K, Woster AP, Goldstein RS & Carlton EJ (2016) Untangling the impacts of climate change on waterborne diseases: a systematic review of relationships between diarrheal diseases and temperature, rainfall, flooding, and drought. Environmental Science & Technology, 50(10), 4905–4922. Available from: 10.1021/acs.est.5b06186 [PubMed: 27058059]

Linden R, Knippertz P, Fink AH, Ingleby B, Maranan M & Benedetti A (2020) The influence of DACCIWA radiosonde data on the quality of ECMWF analyses and forecasts over southern West Africa. Quarterly Journal of the Royal Meteorological Society, 146(729), 1719–1739. Available from: 10.1002/qj.3763

Louve S, Sultan B, Janicot S, Kamsu-Tamo PH & Ndiaye O (2016) Evaulation of TIGGE precipitation forecasts over West Africa at interseasonal time scales. Climate Dynamics, 47, 31–47.

Love TB, Kumar V, Xie P & Thiaw W (2004) P5. 4 a 20-year daily Africa precipitation climatology using satellite and gauge data. In: 14th conference on applied climatology. Boston, MA: American Meteorological Society

Luo L & Wood EF (2006) Assessing the idealized predictability of precipitation and temperature in the NCEP Climate Forecast System. Geophysical Research Letters, 33(4), 1–4.

Ma J, Bowley KA & Zhang F (2019) Evaluating the forecast performance of the meiyu front rainbelt position: a case study of the 30 June to 4 July 2016 extreme rainfall event. Atmosphere, 10(11), 648.

Maidment R, Black E, Greatrex H & Young M (2020) TAMSAT. In: Satellite precipitation measurement. Cham: Springer, pp. 393–407.

Maidment RI, Grimes DIF, Allan RP, Greatrex H, Rojas O & Leo O (2013) Evaluation of satellite-based and model re-analysis rainfall estimates for Uganda: evaluation of rainfall estimates for Uganda. Meteorological Applications, 20(3), 308–317. Available from: 10.1002/met.1283

Maidment RI, Grimes D, Black E, Tarnavsky E, Young M, Greatrex H et al. (2017) A new, long-term daily satellite-based rainfall dataset for operational monitoring in Africa. Scientific Data, 4(1), 170063. Available from: 10.1038/sdata.2017.63 [PubMed: 28534868]

Maranan M, Fink AH & Knippertz P (2018) Rainfall types over southern West Africa: objective identification, climatology and synoptic environment. Quarterly Journal of the Royal Meteorological Society, 144(714), 1628–1648.

Mbouna AD, Tompkins AM, Lenouo A, Asare EO, Yamba EI & Tchawoua C (2019) Modelled and observed mean and seasonal relationships between climate, population density and malaria indicators in Cameroon. Malaria Journal, 18(1), 1–14. [PubMed: 30602373]

McBride JL & Ebert EE (2000) Verification of quantitative precipitation forecasts from operational numerical weather prediction models over Australia. Weather and Forecasting, 15(1), 103c121.

Meynadier R, Bock O, Gervois S, Guichard F, Redelsperger J-L, Agustí-Panareda A et al. (2010) West African Monsoon water cycle: 2. Assessment of numerical weather prediction water budgets. Journal of Geophysical Research: Atmospheres, 115(D19), 1–24. Available from: 10.1029/2010JD013919

Mupangwa W, Walker S & Twomlow S (2011) Start, end and dry spells of the growing season in semi-arid southern Zimbabwe. Journal of Arid Environments, 75(11), 1097–1104. Available from: 10.1016/j.jaridenv.2011.05.011

Ngwa MC, Liang S, Kracalik IT, Morris L, Blackburn JK, Mbam LM et al. (2016) Cholera in Cameroon, 2000–2012: spatial and temporal analysis at the operational (Health District) and sub climate levels. PLoS Neglected Tropical Diseases, 10(11), e0005105. Available from: 10.1371/journal.pntd.0005105 [PubMed: 27855171]

Nicholson SE (2013) The west African Sahel: a review of recent studies on the rainfall regime and its interannual variability. International Scholarly Research Notices, 2013, 32.

Nicholson SE & Klotter DA (2021) Assessing the reliability of satellite and reanalysis estimates of rainfall in equatorial Africa. Remote Sensing, 13(18), 3609.

Nikulin G, Jones C, Giorgi F, Asrar G, Büchner M, Cerezo-Mota R et al. (2012) Precipitation climatology in an ensemble of CORDEX-Africa regional climate simulations. Journal of Climate, 25(18), 6057–6078. Available from: 10.1175/JCLI-D-11-00375.1

Novella NS & Thiaw WM (2013) African rainfall climatology version 2 for famine early warning systems. Journal of Applied Meteorology and Climatology, 52(3), 588–606.

Ogutu GEO, Franssen WHP, Supit I, Omondi P & Hutjes RWA (2017) Skill of ECMWF system-4 ensemble seasonal climate forecasts for East Africa. International Journal of Climatology, 37(5), 2734–2756. Available from: 10.1002/joc.4876

Osgood D & Shirley KE (2012) The value of information in index Insurance for Farmers in Africa. In: Laxminarayan R & Macauley MK (Eds.) The value of information: methodological frontiers and new applications in environment and health. Netherlands: Springer, pp. 1–18. Available from: 10.1007/978-94-007-4839-2_1

Park Y-Y, Buizza R & Leutbecher M (2008) TIGGE: preliminary results on comparing and combining ensembles. Quarterly Journal of the Royal Meteorological Society, 134(637), 2029–2050. Available from: 10.1002/qj.334

Parker DJ & Diop-Kane M (Eds.). (2017) Meteorology of Tropical West Africa: The Forecasters' Handbook. Chichester, UK: Wiley- Blackwell, p. 496.

Pascual M, Cazelles B, Bouma M.j., Chaves L.f. & Koelle K (2008) Shifting patterns: malaria dynamics and rainfall variability in an African highland. Proceedings of the Royal Society B: Biological Sciences, 275(1631), 123–132. Available from: 10.1098/rspb.2007.1068

Paulson JN, Williams BL, Hehnly C, Mishra N, Sinnar SA, Zhang L et al. (2020) Paenibacillus infection with frequent viral coinfection contributes to postinfectious hydrocephalus in Ugandan infants. Science Translational Medicine, 12(563), 1–12. Available from: 10.1126/scitranslmed.aba0565

Pennelly C, Reuter G & Flesch T (2014) Verification of the WRF model for simulating heavy precipitation in Alberta. Atmospheric Research, 135, 172–192.

Sajadi MM, Habibzadeh P, Vintzileos A, Shokouhi S, Miralles-Wilhelm F & Amoroso A (2020) Temperature, Humidity, and Latitude Analysis to Estimate Potential Spread and Seasonality of Coronavirus Disease 2019 (COVID-19). JAMA Network Open, 3(6), e2011834. Available from: 10.1001/jamanetworkopen.2020.1183 [PubMed: 32525550]

Satgé F, Defrance D, Sultan B, Bonnet M-P, Seyler F, Rouché N et al. (2020) Evaluation of 23 gridded precipitation datasets across West Africa. Journal of Hydrology, 581, 124412. Available from: 10.1016/j.jhydrol.2019.124412

Schiff SJ, Ranjeva SL, Sauer TD & Warf BC (2012) Rainfall drives hydrocephalus in East Africa: clinical article. Journal of Neurosurgery: Pediatrics, 10(3), 161–167. Available from: 10.3171/2012.5.PEDS11557 [PubMed: 22768966]

Ssentongo P, Fronterre C, Geronimo A, Greybush SJ, Mbabazi PK, Muvawala J et al. (2021) Pan-African evolution of within and between country COVID-19 dynamics. Proc Natl Acad Sci U S A, 118(28), e2026664118. Available from: 10.1073/pnas.2026664118 [PubMed: 34187879]

Ssentongo P, Muwanguzi AJB, Eden U, Sauer T, Bwanga G, Kateregga G et al. (2018) Changes in Ugandan climate rainfall at the village and forest level. Scientific Reports, 8(1), 3551. Available from: 10.1038/s41598-018-21427-5 [PubMed: 29476058]

Taraphdar S, Mukhopadhyay P, Leung LR & Landu K (2016) Prediction skill of tropical synoptic scale transients from ECMWF and NCEP ensemble prediction systems. Mathematics of Climate and Weather Forecasting, 2(1), 26–42. Available from: 10.1515/mcwf-2016-0002

Tarnavsky E & Bonifacio R (2020) Drought risk management using satellite-based rainfall estimates. In: Levizzani V, Kidd C, Kirschbaum DB, Kummerow CD, Nakamura K & Turk FJ (Eds.) Satellite precipitation measurement, Vol. 2. Switzerland: Springer International Publishing, pp. 1029–1053. Available from: 10.1007/978-3-030-35798-6_28

Tartaglione N (2010) Relationship between precipitation forecast errors and skill scores of dichotomous forecasts. Weather and Forecasting, 25(1), 355–365.

Thiemig V, Rojas R, Zambrano-Bigiarini M, Levizzani V & De Roo A (2012) Validation of satellite-based precipitation products over sparsely gauged African River Basins. Journal of Hydrometeorology, 13(6), 1760–1783. Available from: 10.1175/JHM-D-12-032.1

Thomson MC & Mason SJ (Eds.). (2019) Climate information for public health action. New York, NY: Routledge, Taylor & Francis Group.

Thomson MC, Muñoz ÁG, Cousin R & Shumake-Guillemot J (2018) Climate drivers of vector-borne diseases in Africa and their relevance to control programmes. Infectious Diseases of Poverty, 7(1), 81. Available from: 10.1186/s40249-018-0460-1 [PubMed: 30092816]

Tompkins AM & Feudale L (2010) Seasonal ensemble predictions of west African monsoon precipitation in the ECMWF system 3 with a focus on the AMMA special observing period in 2006. Weather and Forecasting, 25(2), 768–788.

Toté C, Patricio D, Boogaard H, Van der Wijngaart R, Tarnavsky E & Funk C (2015) Evaluation of satellite rainfall estimates for drought and flood monitoring in Mozambique. Remote Sensing, 7(2), 1758–1776.

Vigaud N & Giannini A (2019) West African convection regimes and their predictability from submonthly forecasts. Climate Dynamics, 52(11), 7029–7048.

Vogel P, Knippertz P, Fink AH, Schlueter A & Gneiting T (2018) Skill of global raw and postprocessed ensemble predictions of rainfall over northern tropical Africa. Weather and Forecasting, 33(2), 369–388.

Washington R & Downing TE (1999) Seasonal forecasting of African rainfall: prediction, responses and household food security. The Geographical Journal, 165(3), 255–274. Available from: 10.2307/3060442

Wiersinga WJ, Virk HS, Torres AG, Currie BJ, Peacock SJ, Dance DAB et al. (2018) Melioidosis. Nature Reviews Disease Primers, 4(1), 1–22. Available from: 10.1038/nrdp.2017.107

Xie P & Arkin PA (1996) Analyses of global monthly precipitation using gauge observations, satellite estimates, and numerical model predictions. Journal of Climate, 9(4), 840–858. Available from: 10.1175/1520-0442(1996)009<0840:AOGMPU>2.0.CO;2

Xue Y, De Sales F, Lau WM, Boone A, Feng J, Dirmeyer P et al. (2010) Intercomparison and analyses of the climatology of the West African Monsoon in the West African Monsoon Modeling and Evaluation project (WAMME) first model intercomparison experiment. Climate Dynamics, 35(1), 3–27.

Yang X, Siddique R, Sharma S, Greybush SJ & Mejia A (2017) Postprocessing of GEFS precipitation ensemble reforecasts over the U.S. middle-Atlantic region. Monthly Weather Review, 145, 1641–1658. Available from: 10.1175/MWR-D-16-0251.1

Zhang Q, Körnich H & Holmgren K (2013) How well do reanalyses represent the southern African precipitation? Climate Dynamics, 40, 951–962. Available from: 10.1007/s00382-012-1423-z

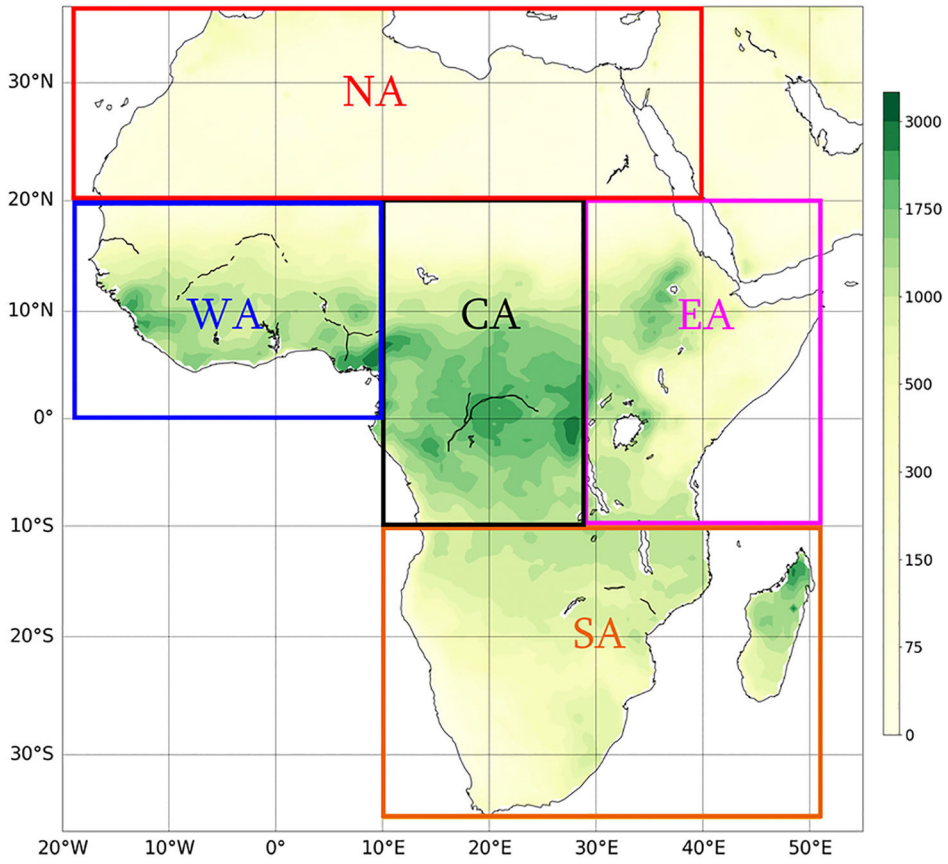

FIGURE 1.

Regions of Africa used in this study: NA, Northern Africa; WA, Western Africa; CA, Central Africa; EA, Eastern Africa; SA, Southern Africa. Background image is a spatial pattern of total RFE2 rainfall (units: mm), summed over 2016–2018.

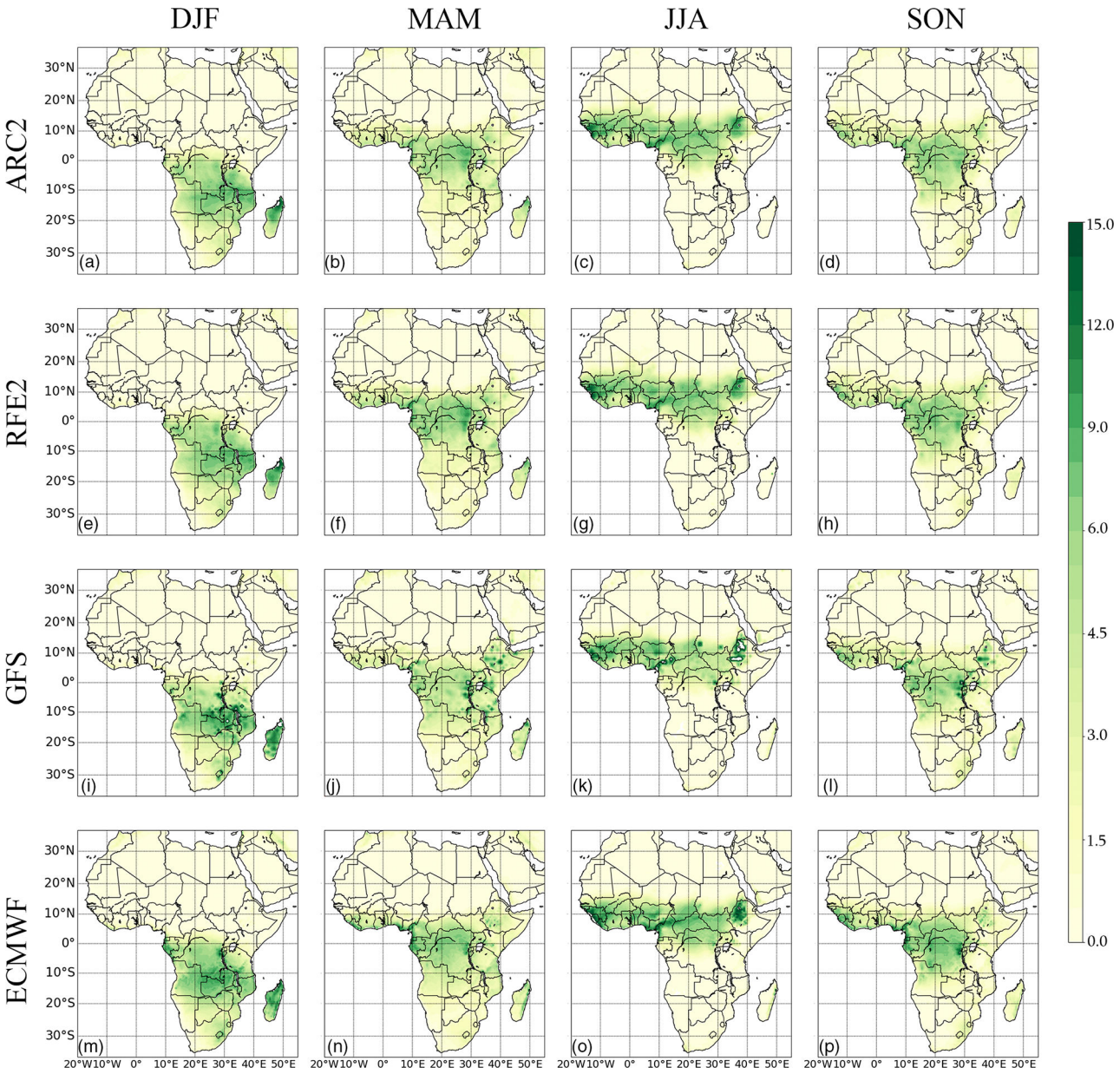

FIGURE 2.

Spatial pattern of averaged daily rainfall, averaged during 2016–2018 (units: mm day^{-1}) of ARC2 (a, b, c, d), RFE2 (e, f, g, h), GFS (i, j, k, l), and ECMWF (m, n, o, p) for each season (December–January–February, DJF (a, e, i, m); March–April–May, MAM (b, f, j, n)); June–July–August, JJA (c, g, k, o); September–October–November, SON (d, h, l, p). The ECMWF and GFS forecasts are at lead time of 1 day.

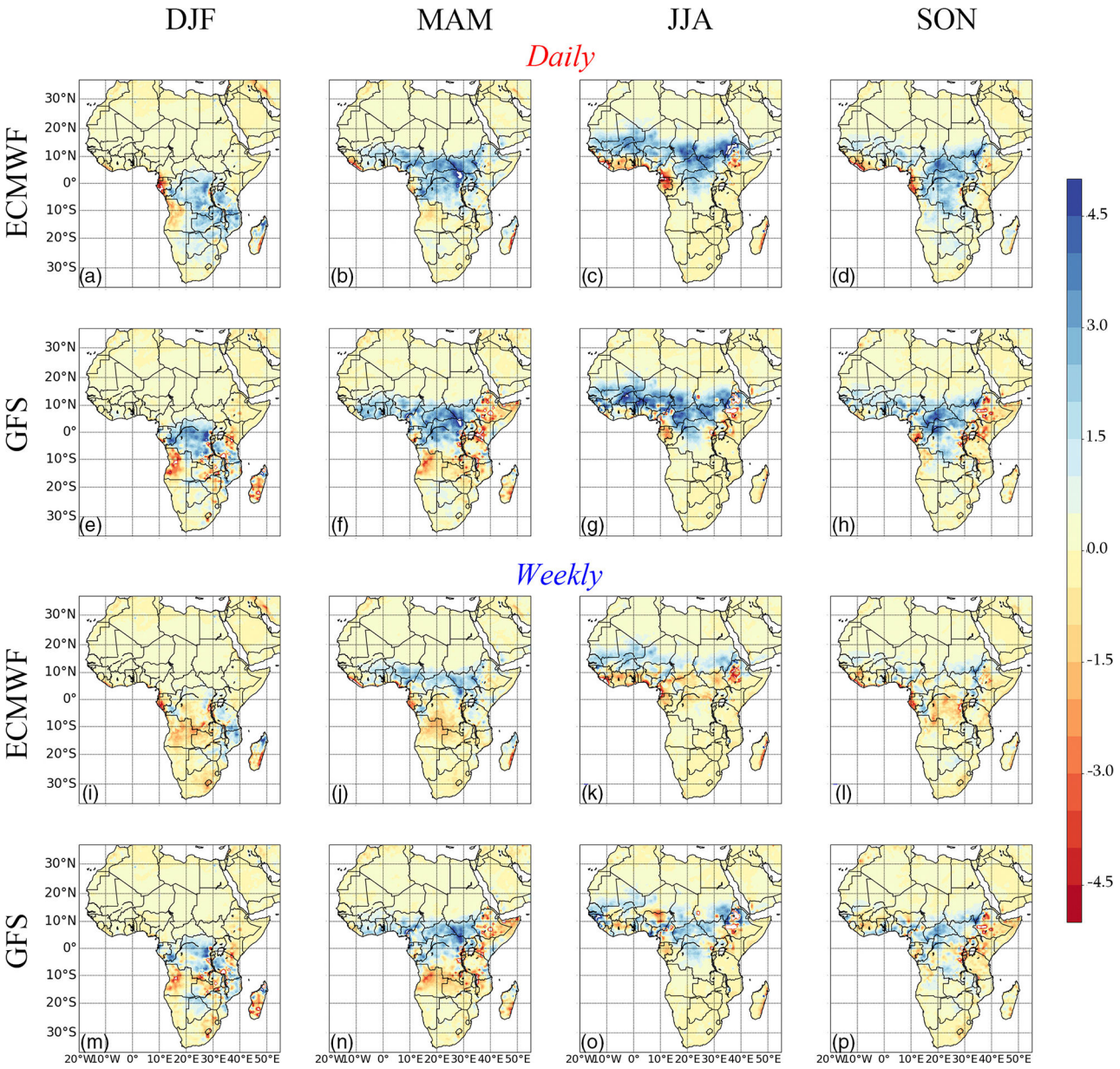

FIGURE 3.

Spatial distribution of Bias (mean observation minus model; units: mm day^{-1}) between NWM forecasts (ECMWF and GFS) and RFE2 observations, at daily and weekly scales, in each season. The NWP forecasts for daily rainfall prediction are at 1 day lead time.

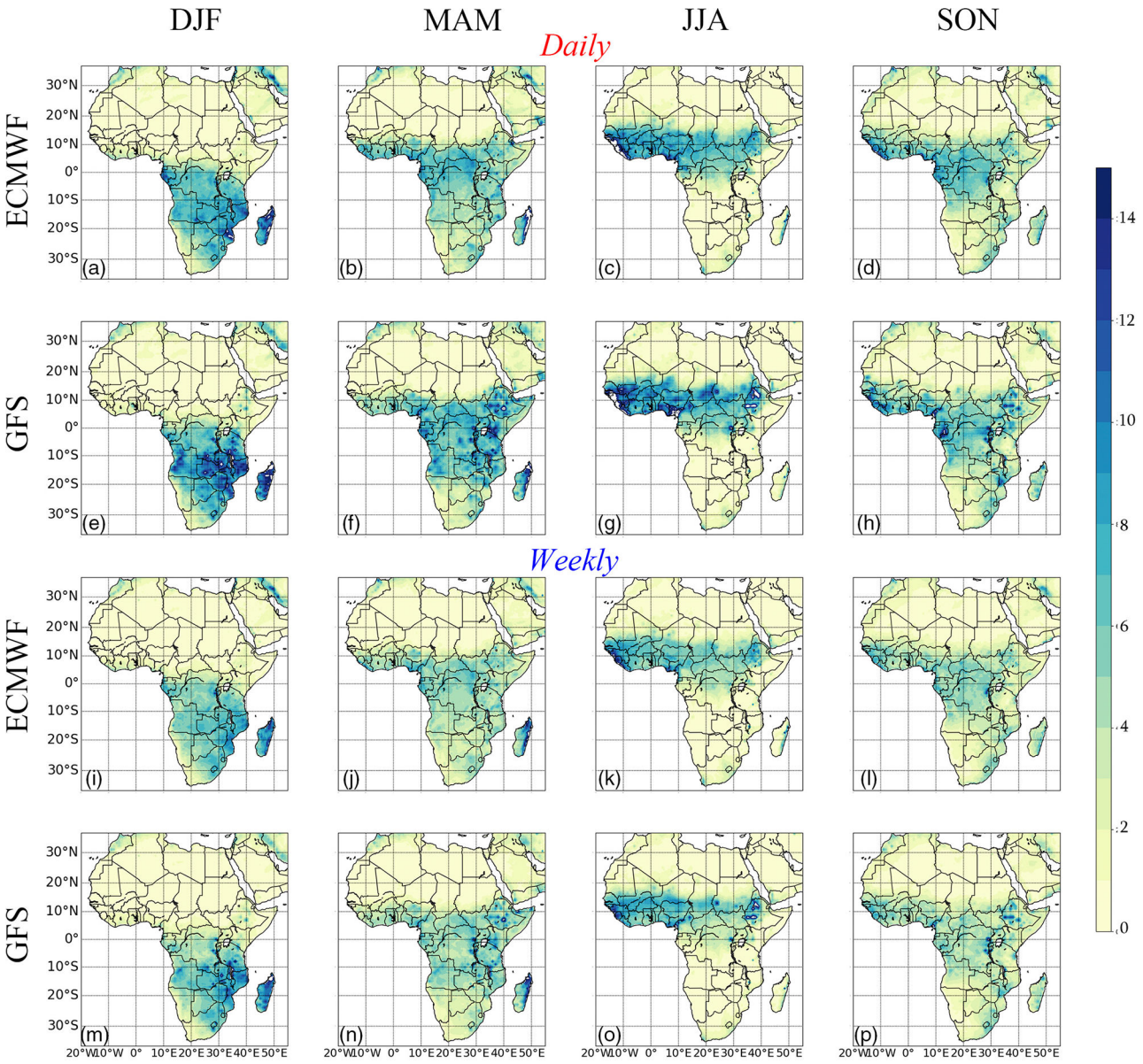

FIGURE 4.

Spatial distribution of RMSE (units: mm day^{-1}) between NWM forecasts (ECMWF and GFS) and RFE2 observations, at daily and weekly scales, in each season. The NWP forecasts for daily rainfall prediction are at 1 day lead time.

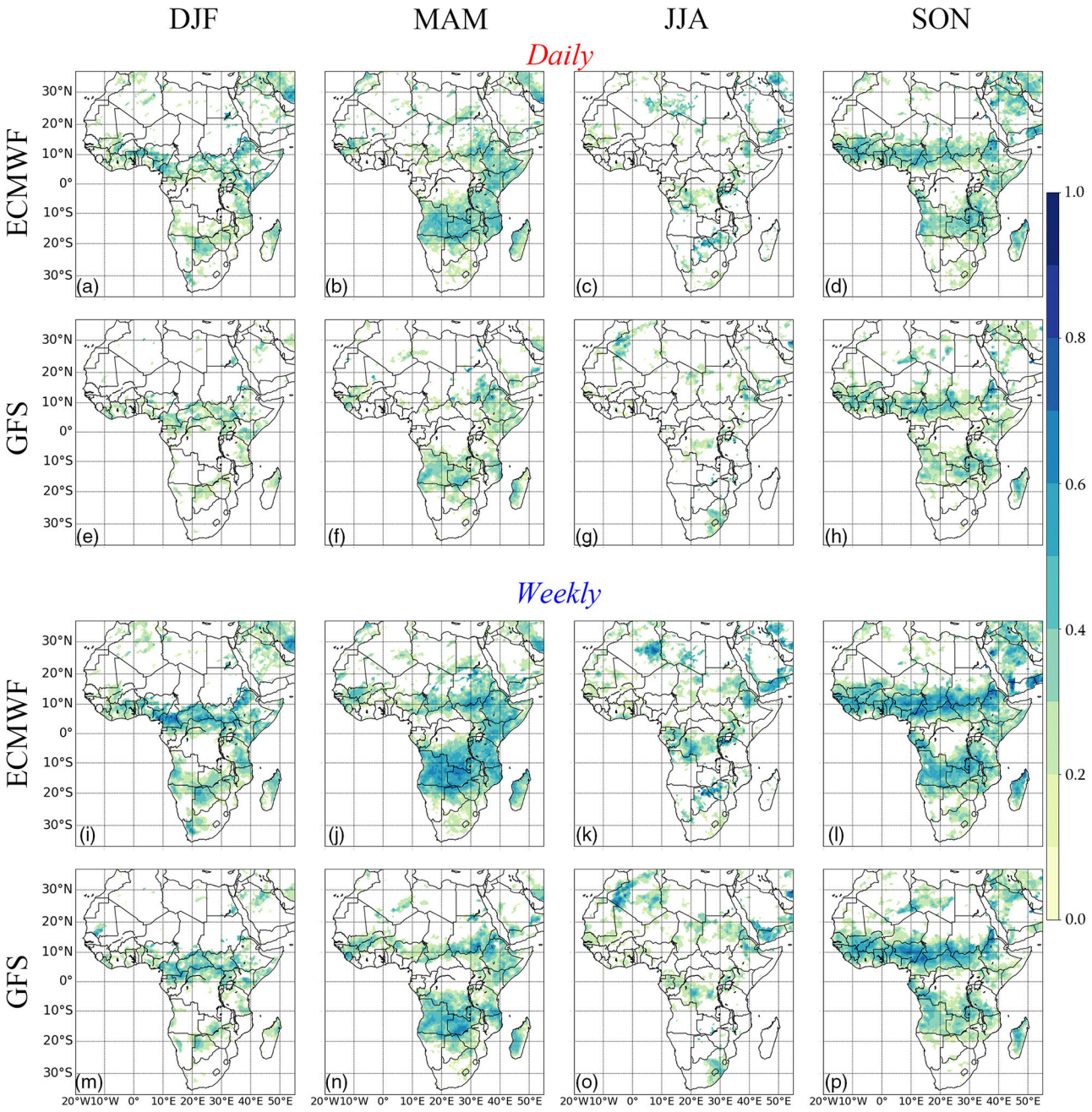

FIGURE 5.

Spatial distributions of correlation coefficient (*r*) between NWM forecasts (ECMWF and GFS) and RFE2 observations, at daily and weekly scales, in each season. The NWP forecasts are at 1 day lead time, and locations with effective days >20 and *p* value <0.01 (indicating positive forecast skill) are shown in colour, hence the colour bar with positive values only.

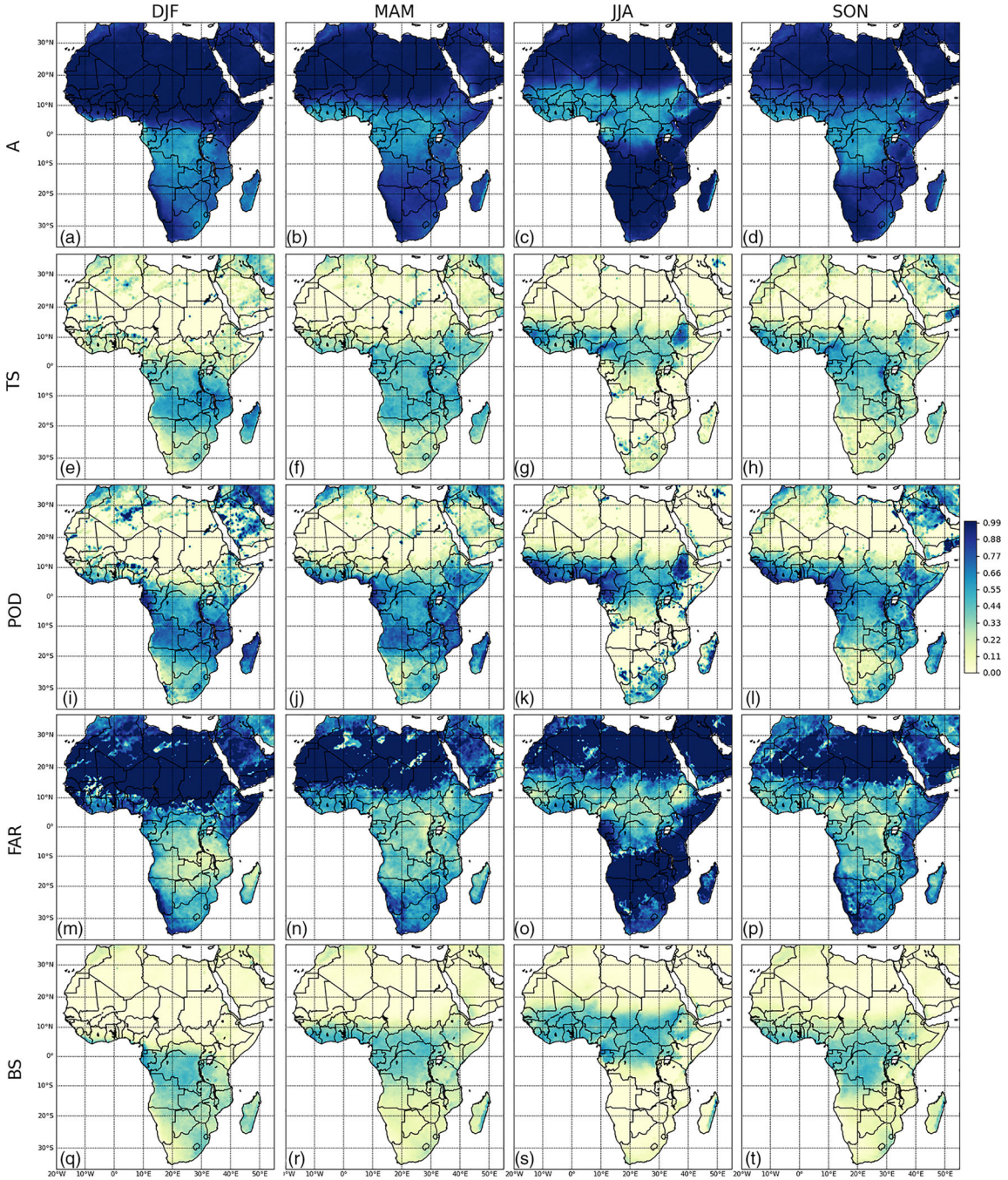

FIGURE 6.

At daily scale, spatial distributions of accuracy (a, b, c, d), threat score (e, f, g, h), probability of detection (i, j, k, l), false alarm rate (m, n, o, p) and Brier score (q, r, s, t) of ECMWF forecasts at 1 day lead time against the RFE2, in each season, during 2016–2018. Threshold is 2 mm day^{-1}.

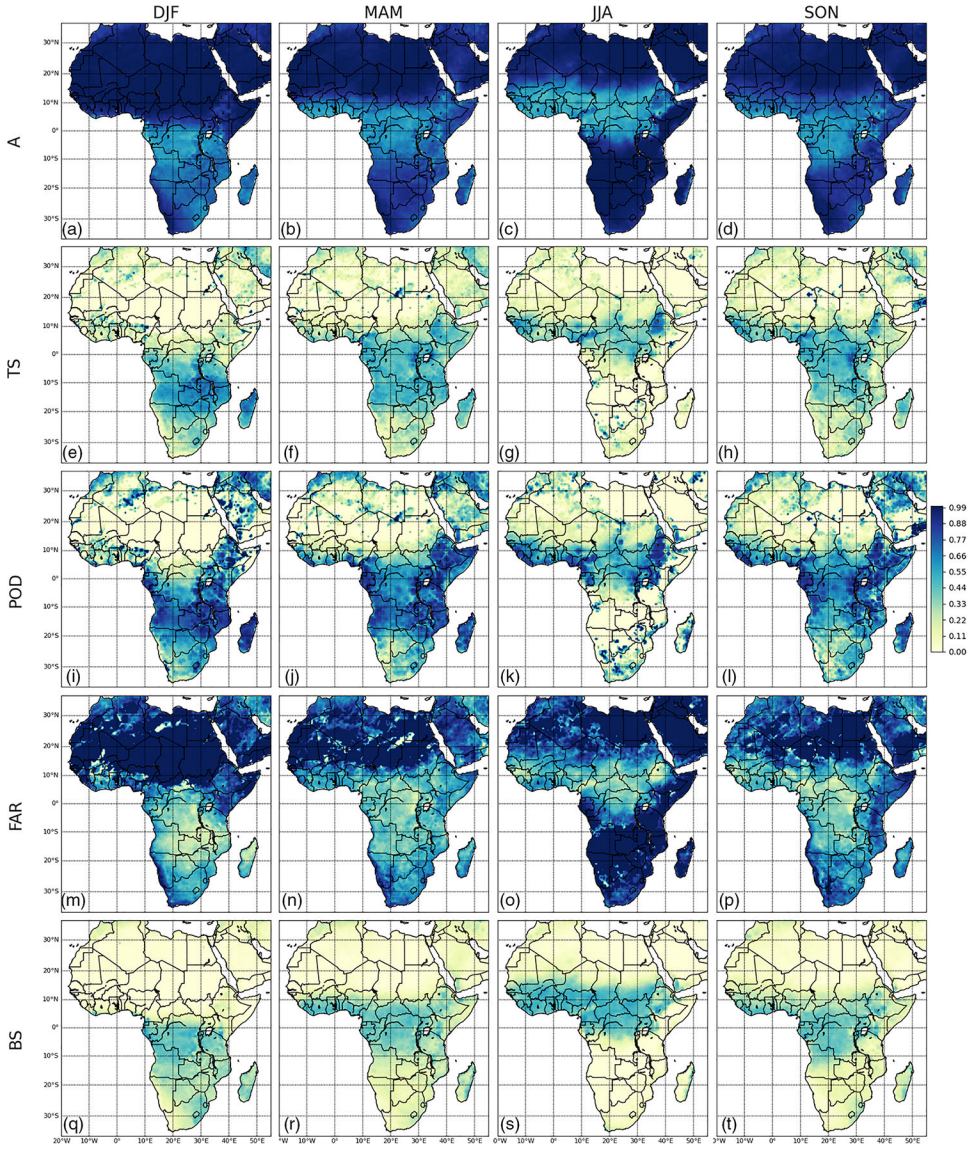

FIGURE 7.

At daily scale, spatial distributions of accuracy (a, b, c, d), threat score (e, f, g, h), probability of detection (i, j, k, l), false alarm rate (m, n, o, p) and Brier Score (q, r, s, t) of GFS forecasts at 1 day lead time against the RFE2, in each season, during 2016–2018. Threshold is 2 mm day^{-1}.

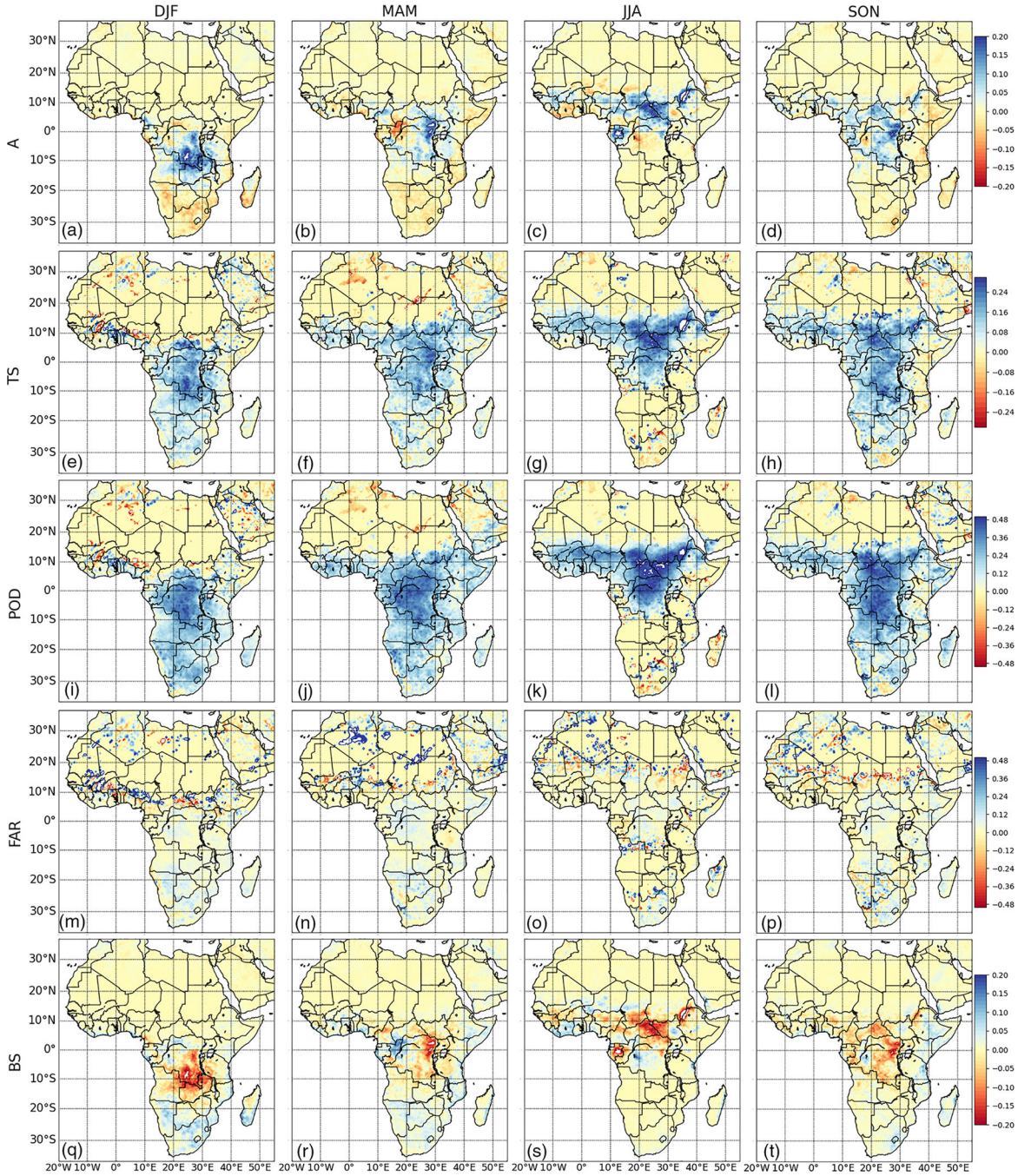

FIGURE 8.

Weekly NWM forecast metrics minus daily forecast metrics. The ECMWF NWM forecasts for daily rainfall prediction are at 1 day lead time. A positive value (blue) indicates an improved performance for weekly versus daily for A, TS and POD; a negative value (red) indicates an improved performance for weekly versus daily for FAR and BS.

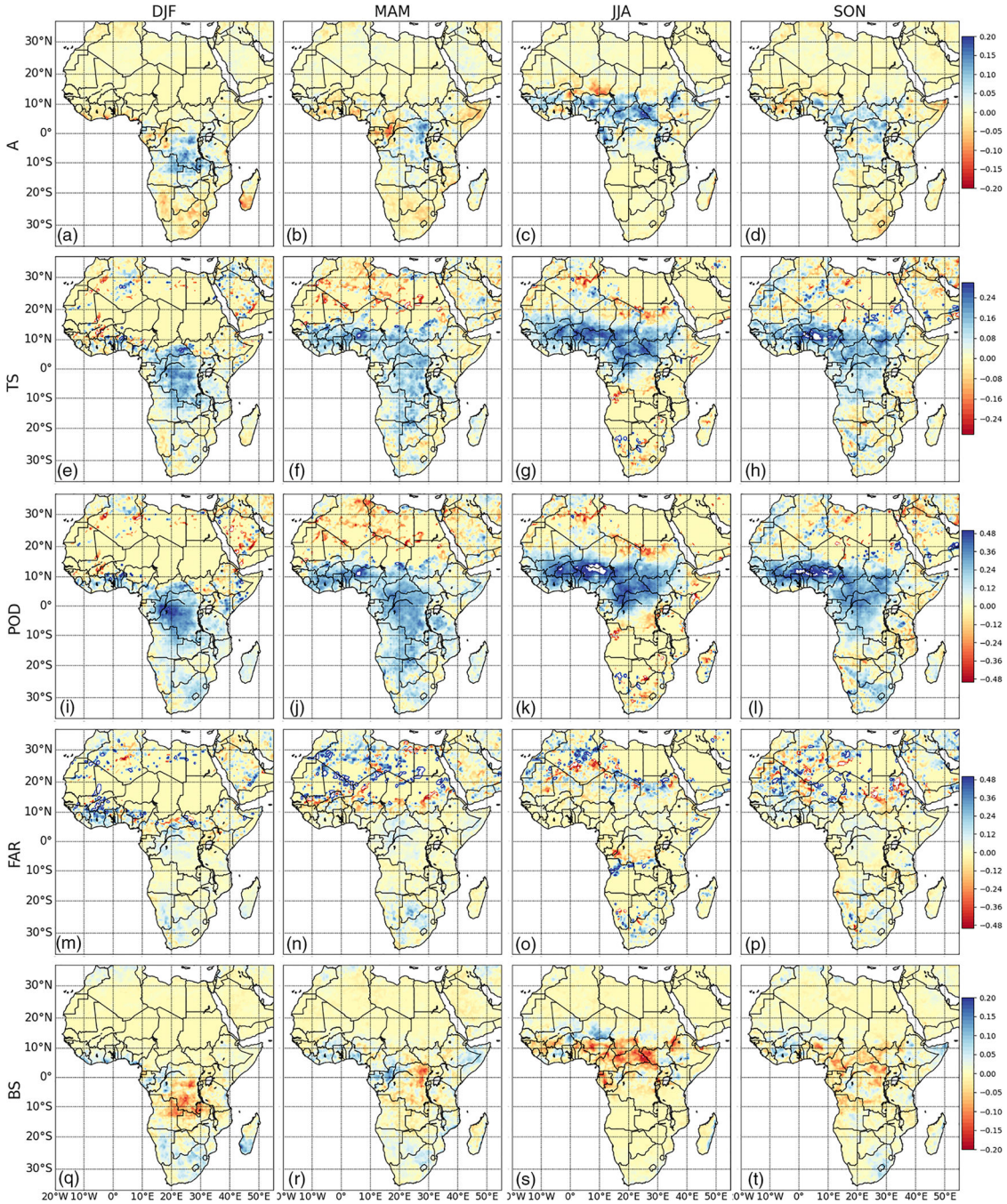

FIGURE 9.

Weekly NWM forecast metrics minus daily forecast metrics. The GFS NWM forecasts for daily rainfall prediction are at 1 day lead time. A positive value (blue) indicates an improved performance for weekly versus daily for A, TS and POD; a negative value (red) indicates an improved performance for weekly versus daily for FAR and BS.

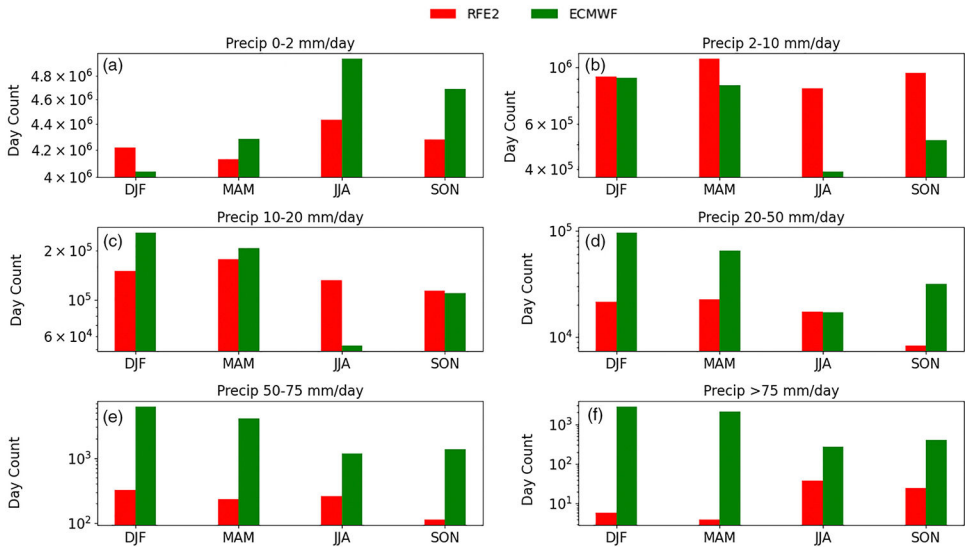

FIGURE 10.

Cumulative number of days over all locations per season for RFE2 (red) and ECMWF (green) rainfall in different intensity ranges: (a) 0–2 mm day^{-1}, (b) 2–10 mm day^{-1}, (c) 10–20 mm day^{-1}, (d) 20–50 mm day^{-1}, (e) 50–75 mm day^{-1}, and (f) >75 mm day^{-1}.

TABLE 1

Main characteristics of the satellite and forecast rainfall data used in this study.

Name	Source	Availability from indicated source	Initialization time (UTC)	Spatial resolution	Temporal resolution
RFE2	ftp://ftp.cpc.ncep.noaa.gov/fews/fewsdata/africa/rfe2/	2001-present	N/A	0.1° × 0.1°	Daily Since 12Z
ARC2	ftp://ftp.cpc.ncep.noaa.gov/fews/fewsdata/africa/arc2/	1983-present	N/A	0.1° × 0.1°	Daily Since 12Z
GFS	https://rda.ucar.edu/datasets/ds084.1/	2015-present	−0000	Native	6- h
			−0600	~13 km	
			−1200	Interpolated	
			−1800	0.5° × 0.5°	
ECMWF	http://apps.ecmwf.int/datasets/data/tigge/levtype=sfc/type=cf/	2006-present	−0000	Native	6-h
			−1200	~9 km	
				Interpolated	
				0.5° × 0.5°	

TABLE 2

Verification metrics list. All metrics are calculated across time (using index i, where N is the total number of times in the dataset), separately at each spatial location (grid cell).

Statistical index	Equation	Range	Perfect value
Bias (subtractive)	$\text{Bias} A = \text{mean}(\text{RF}_i - \text{RS}_i)$	$-\infty$ to ∞	0
Root mean squared error (RMSE)	$\text{RMSE} = \sqrt{\frac{1}{N}\sum(\text{RF}_i - \text{RS}_i)^2}$	0 to ∞	0
Pearson's correlation coefficient (r)	$r = \frac{\sum\left(\text{RF}_i - \bar{\bar{\text{RF}}}\right)\left(\text{RS}_i - \bar{\bar{\text{RS}}}\right)}{\sqrt{\sum\left(\text{RF}_i - \bar{\bar{\text{RF}}}\right)^2 \sum\left(\text{RS}_i - \bar{\bar{\text{RS}}}\right)^2}}$	−1 to 1	1
Accuracy (A); Proportion Correct	$A = \frac{\text{TP} + \text{TN}}{\text{TP} + \text{FP} + \text{FN} + \text{TN}}$	0 to 1	1
Threat score (TS); Critical success Index	$\text{TS} = \frac{\text{TP}}{\text{TP} + \text{FP} + \text{FN}}$	0 to 1	1
False alarm rate (FAR)	$\text{FAR} = \frac{\text{FP}}{\text{TP} + \text{FP}}$	0 to 1	0
Probability of detection (POD)	$\text{POD} = \frac{\text{TP}}{\text{TP} + \text{FN}}$	0 to 1	1
Brier score (BS)	$\text{BS} = \frac{1}{N}\sum(F_i - O_i)^2$	0 1	0

Abbreviations: F_i, the probability that was forecast on day i; FN, false negative, missed event (event was not forecast but did occur in observation); FP, false positive, false alarm (event was forecast, but did not occur in observation); O_i, The actual outcome that was observed on day i; RF_i, rainfall forecast from NWM (unit: Mm day^{-1}) on day i; RS_i, Rainfall observation from satellite (unit: Mm day^{-1}) on day i; TN, True negative, correct negative (event was not forecast and did not occur in observation); TP, True positive, hit (event was forecast and occurred in observations).